

APPLICATION OF NASTRAN TO LARGE DEFLECTION  
SUPERSONIC FLUTTER OF PANELS

by

Chuh Mei  
Vought Corporation, Hampton, Virginia

and

James L. Rogers, Jr.  
NASA-Langley Research Center, Hampton, Virginia

SUMMARY

Flat panel flutter at high supersonic Mach number is analyzed using NASTRAN Level 16.0 by means of modifications to the code. Two-dimensional plate theory and quasi-steady aerodynamic theory are employed. The finite element formulation and solution procedure are presented. Modifications to the NASTRAN code are discussed. Convergence characteristics of the iteration processes are also briefly discussed. Effects of aerodynamic damping, boundary support condition and applied in-plane loading are included. Comparison of nonlinear vibration and linear flutter results with analytical solutions demonstrate that excellent accuracy is obtained with NASTRAN.

INTRODUCTION

Panel flutter is the self-excited oscillation of the external skin of a flight vehicle when exposed to an airflow along its surface. The classic approach using linear structural theory indicates that there is a critical (or flutter) dynamic pressure above which the panel motion becomes unstable. Since the linear theory does not account for structural nonlinearities, it can only determine the flutter boundary and can give no information about the flutter oscillation itself. A great quantity of literature exists on linear panel flutter (e.g. refs. 1 and 2 plus others too numerous to mention).

For large deflections, the nonlinear effects, mainly due to midplane stretching forces, restrain the panel motion to bounded limit cycle oscillations with increasing amplitude as dynamic pressure increases. Therefore, for realistic assessments and understanding of panel flutter, the nonlinear theory should be used. An excellent survey on both linear and nonlinear panel flutter through 1970 is given by Dowell (ref. 3).

To investigate large amplitude panel flutter, a number of approaches can be used. A modal approach with direct numerical integration has been used by Dowell (refs. 4 and 5). The major disadvantage in using this approach is its long computing time. The harmonic balance method can be used to determine limit cycles; see for example, Eastep and McIntosh (ref. 6) and Kuo et. al. (ref. 7). This approach, however, is quite complicated in mathematic manipulations. Morino (refs. 7 and 8) also used the pertubation method to obtain neighboring solutions to the linear problem.

The finite element method has been used successfully in investigating linear panel flutter (refs. 9 to 15). Because of its versatile applicability, effects of aerodynamic damping, complex panel configuration (e.g. delta planform in ref. 11, and rhombic planform in ref. 13), flow angularity, midplane forces, and anisotropic material properties can be conveniently included. Recently, the finite element method has been applied successfully in large amplitude vibrations of beam and plate structures (refs. 16 to 18). Thus, it is logical to extend the finite element application to study the limit cycle oscillations of panels.

The purpose of this paper is to describe a large deflection supersonic panel flutter capability available for NASTRAN Level 16.0 by means of DMAP sequences and modifications of the code. The paper includes a brief discussion of the theoretical formulation and solution procedure. Effects of aerodynamic damping, initial in-plane loading and boundary support condition are included. DMAP sequences required for nonlinear panel flutter analysis and an example of input bulk data are given in the Appendices.

#### SYMBOLS

a	length
[a]	nonsymmetric aerodynamic matrix
$c = (w)_{\max}$	amplitude of oscillation
$D = \frac{Eh^3}{12(1-\nu^2)}$	bending rigidity
[d]	aerodynamic damping matrix
E	modulus of elasticity
{f}	interpolation function

SYMBOLS (CONT'D)

$\xi_A$	aerodynamic damping parameter, equation (21)
$h$	thickness
$i = \sqrt{-1}$	
$[k]$	stiffness matrix
$[k^d]$	differential stiffness matrix
$[k^g]$	geometrical stiffness matrix
$M$	Mach number
$[m]$	mass matrix
$N_x$	inplane force due to deflection, tension positive
$N_{x0}$	applied inplane force, tension positive
$p$	aerodynamic force
$\{Q\}$	generalized aerodynamic force
$q$	dynamic pressure
$t$	time
$\{u\}$	nodal displacements
$V$	flow velocity
$w$	deflection
$x, y, z$	coordinates
$\alpha$	damping factor
$\beta = \sqrt{M^2 - 1}$	
$\epsilon$	norm
$\kappa$	complex eigenvalue, equation (19)
$\lambda = \frac{2qa}{\beta D}^3$	dynamic pressure parameter

## SYMBOLS (CONT'D)

$\mu$		aerodynamic damping coefficient, equation (8)
$\nu$		Poisson's ratio
$\rho$		panel mass density
$\rho_A$		air mass density
$\{\phi\}$		eigenvector
$\Omega = \alpha + i \omega$		response of system
$\omega$		frequency
$\omega_0$		reference frequency
<b>Subscripts:</b>		
aa		analysis
ee		element

## THEORETICAL FORMULATION AND ITS SOLUTION

### Formulation of Matrix Equation of Motion

The panel is represented by a flat thin plate of unit width in bending as shown in figure 1. The transverse dynamic equilibrium equation may be written as:

$$D \frac{\partial^4 w}{\partial x^4} - (N_x + N_{x0}) \frac{\partial^2 w}{\partial x^2} + \rho h \frac{\partial^2 w}{\partial t^2} = p \quad (1)$$

Where

$$N_x = \frac{Eh}{2a} \int_0^a \left( \frac{\partial w}{\partial x} \right)^2 dx \quad (2)$$

is the membrane force induced by large deflections, and  $N_{x0}$  is the initial in-plane loading. For sufficiently high supersonic speeds ( $M > 1.6$ ), the aerodynamic pressure can be described by the two dimensional aerodynamic theory:

$$p(x,y,t) = - \frac{2q}{\beta} \left[ \frac{\partial w}{\partial x} + \frac{1}{V} \frac{M^2-2}{M^2-1} \frac{\partial w}{\partial t} \right] \quad (3)$$

In the finite element method, the stiffness equations of motion for a plate element under the influence of elastic, initial in-plane, large deflection, and inertia forces (ref. 17) with the inclusion of aerodynamic forces may be written as:

$$([k_{ee}] + [k_{ee}^d] + [k_{ee}^g])\{u_e\} + [m_{ee}]\{\ddot{u}_e\} = \{Q(t)\} \quad (4)$$

The stiffness  $[k_{ee}]$ , differential stiffness  $[k_{ee}^d]$ , and mass  $[m_{ee}]$  matrices have been well developed for almost every plate finite element available. The geometrical stiffness matrix  $[k_{ee}^g]$  has been derived in references 16 and 17 for beam and rectangular plate elements. The development of the aerodynamic matrices follows the method proposed by Olson (refs. 9 and 11). The virtual work,  $U$ , of the aerodynamic force is

$$\begin{aligned} U &= Q_j u_j \\ &= \iint p(x,y,t) w \, dx \, dy \end{aligned} \quad (5)$$

Assuming the displacements are exponential functions of time

$$w(x,t) = w(x)e^{\Omega t} \quad (6)$$

where, in general,  $\Omega = \alpha + i\omega$ . Substituting expressions for the aerodynamic pressure, equation (3), and the displacement functions, equation (6), the virtual work becomes

$$U = \left\{ -\frac{2q}{\beta} \int \frac{dw}{dx} w dx - \mu \Omega \int w^2 dx \right\} e^{\Omega t} \quad (7)$$

$$\text{where } \mu = \frac{2q}{v} \frac{M^2 - 2}{\beta^3} \quad (8)$$

The deflection function for a particular element is usually assumed in the form:

$$w(x) = \sum_j f_j(x) u_j = \{f\}^T \{u\} \quad (9)$$

where  $f_j$  is the interpolation function corresponding to the element<sup>j</sup> nodal degree-of-freedom  $u_j$ . Introducing the expression for  $w(x)$ , equation (7) yields

$$U = \left\{ -\frac{2q}{\beta} \{u_e\}^T [a_{ee}] \{u_e\} - \mu \Omega \{u_e\}^T [d_{ee}] \{u_e\} \right\} e^{\Omega t} \quad (10)$$

where

$$[a_{ee}] = \int \left\{ \frac{\partial f}{\partial x} \right\} \{f\} dx \quad (11)$$

is the non-symmetric aerodynamic matrix and

$$[d_{ee}] = \int w^2 dx \quad (12)$$

is the aerodynamic damping matrix. The generalized aerodynamic forces are

$$Q_j = \frac{\partial U}{\partial u_j} = -\left(\frac{2q}{\beta} [a_{ee}] + \mu \Omega [d_{ee}]\right) \{u_e\} e^{\Omega t} \quad (13)$$

and their substitution into equation (4) yields the dynamic equilibrium of the panel in the form:

$$\begin{aligned} & ([k_{ee}] + [k_{ee}^d] + [k_{ee}^g] + \frac{2q}{\beta} [a_{ee}] \\ & + \Omega^2 [m_{ee}] + \mu \Omega [d_{ee}]) \{u_e\} = 0 \end{aligned} \quad (14)$$

The aerodynamic damping matrix, equation (12), can be related to the mass matrix by the expression:

$$[d_{ee}] = \frac{1}{\rho h} [m_{ee}] \quad (15)$$

and equation (14) takes the final form for a finite element as,

$$\begin{aligned} & ([k_{ee}] + [k_{ee}^d] + [k_{ee}^g] + \frac{2q}{\beta} [a_{ee}] \\ & + \Omega^2 [m_{ee}] + \frac{\mu \Omega}{\rho h} [m_{ee}]) \{u_e\} = 0 \end{aligned} \quad (16)$$

#### Solution Procedure

Assembling the finite elements, applying the kinematic boundary conditions, and dividing by  $(\frac{D}{a^3})$  equation (16) leads to a nondimen-

sional eigenvalue problem of the form:

$$([k_{aa}] + [k_{aa}^d] + [k_{aa}^g] + \lambda [a_{aa}] - \kappa [m_{aa}]) \{u_a\} = 0 \quad (17)$$

where

$$\lambda = \frac{2qa^3}{\beta D} \quad (18)$$

and

$$\kappa = -\frac{\rho ha^4}{D} \Omega^2 - \lambda \frac{M^2 - 2}{\beta^2} \frac{a}{V} \Omega \quad (19)$$

are the nondimensional dynamic pressure parameter and eigenvalues, respectively. The eigenvalues can be put into more convenient form as

$$\kappa = -\frac{\Omega^2}{\omega_o^2} - g_A \frac{\Omega}{\omega_o} \quad (20)$$

where

$$g_A = \frac{M^2 - 2}{\beta^3} \frac{\rho V}{\rho h \omega_o} \quad (21)$$

is the nondimensional aerodynamic damping parameter, and

$$\omega_o = \sqrt{\frac{D}{\rho ha^4}} \quad (22)$$



is a convenient frequency scale. For typical panels,  $g_A$  ranges from 0 to 50 approximately, as given in figure 2 of reference 2.

In determining the eigenvalues  $\kappa$  in equation (17) for a given dynamic pressure  $\lambda$ , the iterative procedure and equivalent linearization technique discussed in detail in reference 17 was employed. A simple flow diagram of the procedure is shown in figure 2. The solution procedure is illustrated briefly as follows. For a given  $\lambda$ , first the linear flutter problem is solved

$$\kappa [m_{aa}] \{\phi\}_0 = ([k_{aa}] + [k_{aa}^d] + \lambda [a_{aa}]) \{\phi\}_0 \quad (23)$$

where  $\{\phi\}_0$  represents the linear mode shape normalized by its maximum components. The first approximate displacement is then expressed in the form

$$\{u_a\}_1 = c \text{Real}(\{\phi\}_0 e^{(\alpha + i\omega)t}) \quad (24)$$

where  $c$  is a given amplitude of panel oscillations, and  $\alpha$  and  $\omega$  are the panel response parameters related to  $\kappa$  and  $g_A$  by equation (30). An equivalent geometrical stiffness matrix  $[k_{aa}^g]_{eq}$  now can be obtained using  $\{u_a\}_1$ , and equation (17) is approximated by a linearized eigenvalue equation of the form

$$\kappa [m_{aa}] \{\phi\}_1 = ([k_{aa}] + [k_{aa}^d] + [k_{aa}^g]_{eq} + \lambda [a_{aa}]) \{\phi\}_1 \quad (25)$$

where  $\kappa$  is the eigenvalue associated with amplitude  $c$ , and  $\{\phi\}_1$  is the corresponding mode shape. The iterative process can be repeated until a convergence criterion is satisfied as shown in figure 2. The maximum displacement norm convergence criterion proposed in reference 19 was used in the present study and is defined as

$$\|\epsilon\|_u = \max_j \left| \frac{\Delta u_j}{u_{j,ref}} \right| \quad (26)$$

where  $\Delta u_j$  is the change in displacement component  $j$  during iteration cycle  $n$ ,  $u_{j,ref}$  is the reference displacement. The reference displacement  $u_{j,ref}$  is the largest displacement component of the corresponding "type". For instance in a panel flutter problem involving deflections and rotations, the reference displacement is the largest deflection component and the largest rotation, respectively. In addition a frequency norm is also introduced in the present study and is defined as

$$\| \epsilon \|_f = \left| \frac{\Delta \kappa_n}{\kappa_n} \right| \quad (27)$$

where  $\Delta \kappa_n$  is the change in eigenvalue during iteration cycle  $n$ .

A typical plot of the maximum and frequency norms versus number of iterations for a simply supported panel is shown in figure 3. A modified absolute norm and a modified Euclidean norm defined in reference 19 were also calculated. They fall in between the maximum and frequency norms, and therefore, are not plotted on the figure. In the examples presented in the following section, convergence is considered achieved whenever any one of the norms reaches a value of  $10^{-3}$ .

Equation (17) indicates that when  $\lambda=0$  the problem degenerates into large amplitude vibrations of invacuo panels. The matrices  $[k]$ ,  $[k^d]$ ,  $[k^g]$ , and  $[m]$  are all symmetric and the eigenvalues are real and positive. As  $\lambda$  is increased from zero, two of these eigenvalues will usually approach each other and coalesce to  $\kappa_{cr}$  at  $\lambda = \lambda_{cr}$ , and become complex conjugate pairs

$$\kappa = \kappa_R \pm i \kappa_I \quad (28)$$

for  $\lambda > \lambda_{cr}$ . Here  $\lambda_{cr}$  is considered to be the lowest value of  $\lambda$  for which coalescence occurs among all limit cycle amplitudes and usually corresponds to  $c = 0$ . A typical plot of  $\kappa$  versus  $\lambda$  is shown in figure 4. In the absence of aerodynamic damping ( $g_A = 0$ ), the flutter boundary simply corresponds to  $\lambda_{cr}$ . When  $\lambda$  is below  $\lambda_{cr}$ , any disturbance to the panel decays and  $\kappa_{cr}(c/h) \rightarrow 0$ .

For  $\lambda > \lambda_{cr}$ , a periodic limit cycle oscillation exists which increases in amplitude as  $\lambda$  increases. This can be seen more clearly by noting that the eigenvalue with a negative imaginary part leads to an instability (see ref. 13) and relating the complex eigenvalues to the panel response parameters  $\alpha$  and  $\omega$  as follows. Rewrite equations (20) and (28) as

$$\left(\frac{\Omega}{\omega_0}\right)^2 + g_A \frac{\Omega}{\omega_0} + (\kappa_R - i \kappa_I) = 0 \quad (29)$$

which can be solved for  $\Omega$  to give

$$\begin{aligned} \frac{\Omega}{\omega_0} &= \frac{\alpha}{\omega_0} + i \frac{\omega}{\omega_0} \\ &= \left(-\frac{g_A}{2} + \psi\right) + i \left(\frac{\kappa_I}{2\psi}\right) \end{aligned} \quad (30)$$

where

$$\psi = \pm \frac{1}{\sqrt{2}} \left\{ \sqrt{\left[\left(\frac{g_A}{2}\right)^2 - \kappa_R\right]^2 + \kappa_I^2} + \left[\left(\frac{g_A}{2}\right)^2 - \kappa_R\right] \right\}^{1/2} \quad (31)$$

The complete panel behavior is characterized by plotting the variation of  $\alpha + i\omega$  with increasing dynamic pressure  $\lambda$ . Amplitude increases when  $\alpha$  becomes positive. A typical plot is shown in figure 5.

#### MODIFICATIONS TO THE NASTRAN CODE

To incorporate this new capability into NASTRAN, four existing NASTRAN subroutines must be modified. These subroutines are DBAR, KBAR, SDR1A (SDR1AZZ on CDC computers because of multiple entry points), and XMPLBD. DBAR was modified in the same way as shown in reference 17.

Subroutine KBAR was modified to calculate the aerodynamic matrix  $[a_{ee}]$ . This matrix is multiplied by the parameter  $DPMN = 2q/\beta$ .

DPMN is input via a PARAM card in the BULK DATA deck. DPMN is passed to KBAR through blank common from module EMG. The new EMG calling sequence allowing for the DPMN parameter is shown as follows:

EMG EST,CSTM,MPT,DIT,GEOM2,/KELM,KDICT,MELM,MDICT,,/V,N,NOKGGX/ V,  
 N,NOMGG/C,N,/C,N,/C,N,/C,Y,COUPMASS/C,Y,CPBAR/C,Y,CPROD/C,Y,  
 CPQUAD1/C,Y,CPQUAD2/C,Y,CPTRIA1/C,Y,CPTRIA2/ C,Y,CPTUBE/C,Y,  
 CPQDPLT/C,Y,CPTRPLT/C,Y,CPTRBSC/V,Y,DPMN \$

The default value for DPMN, which is set in XMPLBD, is zero (0). This means if the PARAM card for DPMN is omitted,  $[a_{ee}]$  will make no contribution in equation (14).

Subroutine SDR1A was modified to calculate the real part of  $\{\phi\}_n e^{(\alpha + i\omega)t}$  where  $\{\phi\}_n$  is the complex eigenvector generated by the module CEAD. To avoid entering the modified section of code each time SDR1A is called, a new parameter, IFLUT, was added to the DMAP calling sequence for module SDR1. The contents of IFLUT are passed through blank common from SDR1 to SDR1A. The default value for IFLUT, which is set in XMPLBD, is zero (0). When IFLUT = 0, the new code in SDR1A will not be executed. To set IFLUT = 1 and execute the new code in SDR1A, the following calling sequence for the SDR1 module is used:

SDR1 USET,PHIA,,,G0,GM,KFS/PHIG,, BQG/1/\*REIG\*/1 \$

The underlined parameter sets IFLUT to 1.

Once the changes were made to DBAR, KBAR, SDR1A, and XMPLBD, they were compiled and replaced the old DBAR, KBAR, SDR1A, and XMPLBD in the NASTRAN object library. Link 1, Link 3, Link 12, and Link 13 were relinked, creating a new executable NASTRAN. Although this procedure was done on a CDC computer, similar procedures will produce similar results on the IBM and UNIVAC computers.

To use this capability in NASTRAN, the DMAP sequence shown in Appendix A must be used. This sequence uses many of the new DMAP convenience features in Level 16 of NASTRAN. One of the features allows the REPT module to have a variable parameter. The variable parameter  $NL\phi\phi$  is used for REPT in this DMAP sequence.  $NL\phi\phi$  is input on a PARAM card in the BULK DATA deck. It sets the maximum number of iterations of the inner loop shown in figure 2. The only other input required to use this capability is the addition of another PARAM card in the BULK DATA deck. The parameter AMP corresponds to c and is used to specify the amplitude of vibration of this structure. This capability was added to an in-house version only and is not available in any standard NASTRAN level.

## RESULTS AND DISCUSSION

The large deflection panel flutter analysis developed for use with NASTRAN has been applied to various panels. A typical BULK DATA deck for a simply supported panel at  $\frac{c}{h} = 0.6$  and  $\lambda = 600.0$  is given in Appendix B.

### Convergence Study

Numerical results for the first two eigenvalues at  $\lambda = 0$  and for the coalescence for a simply supported panel and a clamped panel are shown in Table 1. The exact results for eigenvalue coalescence are from reference 20. It is seen that an excellent approximation to the exact results is obtained with only eight elements.

The influence of large deflections on in-vacuo frequencies for a simply supported panel is given in Table 2. Analytical solutions using three different approaches from reference 21 are also given. Comparison of the NASTRAN results with the reference 21 methods show that the eight-element approximation gives very good results. Therefore, eight elements were used in modeling the panels in all the flutter results presented.

### Simply Supported Panel and Effect of Aerodynamic Damping

Plots of the eigenvalues versus dynamic pressure for a simply supported panel at two different panel amplitudes  $\frac{c}{h} = 0.0$  (linear theory) and  $0.6$ , are shown in figure 4. The complete panel behavior is characterized by plotting the  $(\alpha + i\omega)$  variation with increasing dynamic pressure  $\lambda$ , using equation (30) and figure 4, as shown in figure 5. For the case of negligible aerodynamic damping,  $g_A \rightarrow 0$ , instability does not set in until after the two undamped natural frequencies have merged. If some damping is present, the instability sets in at a somewhat higher value as indicated in figure 5. This occurs when  $\alpha = 0$  in equation (30). By routine algebraic manipulation, this instability occurs at the value of  $\lambda$  when

$$g_A = \frac{k_I}{\sqrt{k_R}} \quad (32)$$

and the corresponding limit cycle frequency is

$$\frac{\omega}{\omega_0} = \sqrt{k_R} \quad (33)$$

However, as discussed earlier, this instability is not catastrophic. The panel response does not grow indefinitely, but rather a limit cycle oscillation is developed with increasing amplitude as  $\lambda$  increases.

#### Boundary Support Effect

In figure 6, the panel amplitude of the limit cycle oscillation is given as a function of  $\lambda$  for various panel edge restraints. The most interesting result is that the limit cycle motions are different for hinged-clamped and clamped-hinged panels. This occurs because the aerodynamic matrices are different for the two support conditions, which leads to different deflection shapes for the panels as well as different geometrical stiffness matrices.

#### Effect of In-Plane Loading

Panel amplitude versus  $\lambda$  for several applied in-plane forces acting on a simply supported panel is shown in figure 7. The classical Euler buckling load for simply supported panels is  $N_{cr} = -\pi^2 D/a^2$ . The total membrane force is composed of the applied in-plane load  $N_x$  and the membrane force  $N_x^o$  induced by large deflections of the panel. Figure 7 shows that the applied compressive in-plane force reduces the critical dynamic pressure. However, as the dynamic pressure is increased the panel amplitude increases, which induces tensile in-plane forces that counteract the applied compressive forces. This process continues until a flutter dynamic pressure is reached which corresponds to a given limit cycle amplitude.

#### CONCLUDING REMARKS

A large amplitude supersonic panel flutter capability has been developed for use with NASTRAN Level 16.0 by means of DMAP sequences and modifications to the code. An aerodynamic matrix for a two-dimensional plate element has been developed for NASTRAN by modifying subroutine KBAR. The iteration process has been implemented in NASTRAN through PARAM NL00P in bulk data deck, modifications in subroutines DBAR, KBAR, and SDR1AZZ, and the DMAP sequences. Examples which include effects of aerodynamic damping, applied inplane forces and various support conditions have demonstrated the versatility of the method.

APPENDIX A  
DMAP SEQUENCES

```

ID          NLPF,TWOD
APP         DMAP
BEGIN      $
XDMAP      GO,ERR=2,LIST.
FILE       LAMA=APPEND/PHIA=APPEND $
GP1        GEOM1,GEOM2,/GPL,EQEXIN,GPDT,CSTM,BGPDT,SIL/V,N,LUSET/ V,N,
           NOGPDT $
SAVE       LUSET $
CHKPNT     GPL,EQEXIN,GPDT,CSTM,BGPDT,SIL $
GP2        GEOM2,EQEXIN/ECT $
CHKPNT     ECT $
PARAML     PCDB//C,N,PRES/C,N,/C,N,/C,N,/V,N,NOPCDB $
PURGE      PLTSETX,PLTPAR,GPSETS,ELSETS/NOPCDB $
COND       P1,NOPCDB $
PLTSET     PCDB,EQEXIN,ECT/PLISEIX,PLIPAR,GPSETS,ELSETS/V,N,NSIL/ V,N,
           JUMPPLOT=-1 $
SAVE       NSIL,JUMPPLOT $
PRTMSG     PLTSETX// $
PARAM      //C,N,MPY/V,N,PLTFLG/C,N,1/C,N,1 $
PARAM      //C,N,MPY/V,N,PFILE/C,N,0/C,N,0 $
COND       P1,JUMPPLOT $
PLOT       PLTPAR,GPSETS,ELSETS,CASECC,BGPDT,EQEXIN,SIL,,,,/PLOTX1/ V,N,
           NSIL/V,N,LUSET/V,N,JUMPPLOT/V,N,PLTFLG/V,N,PFILE $
SAVE       JUMPPLOT,PLTFLG,PFILE $
PRTMSG     PLOTX1// $
LABEL      P1 $
CHKPNT     PLTPAR,GPSETS,ELSETS $
GP3        GEOM3,EQEXIN,GEOM2/SLT,GPTT/V,N,NOGRAV $
CHKPNT     SLT,GPTT $
TA1        ECT,ÉPT,BGPDT,SIL,GPTT,CSIM/EST,GEI,GPECTI,/V,N,LUSET/ V,N,
           NOSIMP/C,N,1/V,N,NOGENL/V,N,GENEL $
SAVE       NOSIMP,NOGENL,GENEL $
COND       ERROR1,NOSIMP $
PURGE      OGPST/GENEL $
CHKPNT     EST,GPECT,GEI,OGPST $
PARAM      //C,N,ADD/V,N,NOKGGX/C,N,1/C,N,0 $
PARAM      //C,N,ADD/V,N,NOMGG/C,N,1/C,N,0 $
EMG        EST,CSTM,MPT,DIT,GEOM2,/KELM,KDICT,MELM,MDICT,,/V,N,NOKGGX/ V,
           N,NOMGG/C,N,/C,N,/C,N,/C,Y,COUPMASS/C,Y,CPBAR/C,Y,CPROD/C,Y,
           CPQUAD1/C,Y,CPQUAD2/C,Y,CPTRIA1/C,Y,CPTRIA2/ C,Y,CPIUBE/C,Y,
           CPQDPLT/C,Y,CPTRPLT/C,Y,CPIRBSVC/V,Y,DPMN $
SAVE       NOKGGX,NOMGG $
CHKPNT     KELM,KDICT,MELM,MDICT $
COND       JMPKGG,NOKGGX $

```

EMA GPECT,KDICT,KELM/KGGX,GPST \$  
 CHPNT KGGX,GPST \$  
 LABEL JMPKGG \$  
 COND ERRORS,NOMGG \$  
 EMA GPECT,MDICT,MELM/MGG,/C,N,-1/C,Y,WTMASS=1.0 \$  
 CHPNT MGG \$  
 COND LBL1,GRDPNT \$  
 GPWG BGPDT,CSTM,EGEXIN,MGG/OGPWG/V,Y,GRDPNT/C,Y,WIMASS \$  
 OFF OGPWG,,,,,//\$ \$  
 LABEL LBL1 \$  
 EQUIV KGGX,KGG/NOGENL \$  
 CHPNT KGG \$  
 COND LBL11,NOGENL \$  
 SMA3 GEI,KGGX/KGG/V,N,LUSET/V,N,NOGENL/V,N,NOSIMP \$  
 CHPNT KGG \$  
 LABEL LBL11 \$  
 PARAM //C,N,MPY/V,N,NSKIP/C,N,0/C,N,0 \$  
 GP4 CASECC,GEOM4,EGEXIN,SIL,GPDI,BGPDI,CSIM/RG,YS,USEI,ASEI/V,N,  
 LUSET/V,N,MPCF1/V,N,MPCF2/V,N,SINGLE/V,N,OMI1/V,N,REACT/V,N,  
 NSKIP/V,N,REPEAT/V,N,NOSET/V,N,NOL/V,N,NOA/C,Y,SUBID \$  
 SAVE MPCF1,MPCF2,SINGLE,OMIT,REACT,NSKIP,REPEAT,NOSET,NOL,NOA \$  
 COND ERROR6,NOL \$  
 PARAM //C,N,AND/V,N,NOSR/V,N,SINGLE/V,N,REACT \$  
 PURGE GM/MPCF1/GO,KOO,LOO,PO,UOOV,RUOV/OMIT/PS,KFS,KSS/SINGLE/ QG/  
 NOSR \$  
 CHPNT GM,RG,GO,KOO,LOO,PO,UOOV,RUOV,YS,PS,KFS,KSS,USET,ASET,QG \$  
 COND LBL4D,REACT \$  
 JUMP ERROR2 \$  
 LABEL LBL4D \$  
 COND LBL4,GENEL \$  
 GPSP GPL,GPST,USET,SIL/OGPST/V,N,NOGPST \$  
 SAVE NOGPST \$  
 COND LBL4,NOGPST \$  
 OFF OGPST,,,,,//\$ \$  
 LABEL LBL4 \$  
 EQUIV KGG,KNN/MPCF1/MGG,MNN/MPCF1 \$  
 CHPNT KNN,MNN \$  
 COND LBL2,MPCF2 \$  
 MCE1 USET,RG/GM \$  
 CHPNT GM \$  
 MCE2 USET,GM,KGG,MGG,, /KNN,MNN,, \$  
 CHPNT KNN,MNN \$  
 LABEL LBL2 \$  
 EQUIV KNN,KFF/SINGLE/MNN,MFF/SINGLE \$



CHKPNT KFF,MFF \$  
 COND LBL3,SINGLE \$  
 SCE1 USET,KNN,MNN,,/KFF,KFS,KSS,MFF,, \$  
 CHKPNT KFS,KSS,KFF,MFF \$  
 LABEL LBL3 \$  
 EQUIV KFF,KAA/OMIT/MFF,MAA/OMIT \$  
 CHKPNT KAA,MAA \$  
 COND LBL5,OMIT \$  
 SMP1 USET,KFF,,,/GO,KAA,KOO,LOO,UOO,,,, \$  
 CHKPNT GO,KAA,KOO,LOO,UOO \$  
 SMP2 USET,GO,MFF/MAA \$  
 CHKPNT MAA \$  
 LABEL LBL5 \$  
 RBMG2 KAA/LLL \$  
 CHKPNT LLL \$  
 SSG1 SLT,BGPD,CSTM,SIL,EST,MPT,GPTT,EDT,MGG,CASECC,DIT/PG/ V,N,  
 LUSET/C,N,1 \$  
 CHKPNT PG \$  
 EQUIV PG,PL/NOSET \$  
 CHKPNT PL \$  
 COND LBL10,NOSET \$  
 SSG2 USET,GM,YS,KFS,GO,,PG/,PO,PS,PL \$  
 CHKPNT PO,PS,PL \$  
 LABEL LBL10 \$  
 SSG3 LLL,KAA,PL,LOO,KOO,PO/ULV,UOOV,RULV,RUOV/V,N,OMIT/V,Y,IRES=-1/  
 C,N,1/V,N,EPSI \$  
 SAVE EPSI \$  
 CHKPNT ULV,UOOV,RULV,RUOV \$  
 COND LBL9,IRES \$  
 MATGPR GPL,USET,SIL,RULV//C,N,L \$  
 MATGPR GPL,USET,SIL,RUOV//C,N,0 \$  
 LABEL LBL9 \$  
 SDR1 USET,PG,ULV,UOOV,YS,GO,GM,PS,KFS,KSS,/UGV,PGG,GG/C,N,1/C,N,  
 BKLO \$  
 CHKPNT UGV,GG,PGG \$  
 SDR2 CASECC,CSTM,MPT,DIT,EQEXIN,SIL,GPTT,EDT,BGPD,,QG,UGV,EST,,PGG/  
 OPG1,QQG1,OUGV1,OES1,DEF1,PUGV1/C,N,BKLO \$  
 PARAM //C,N,MPY/V,N,CARDNO/C,N,0/C,N,0 \$  
 OFF OUGV1,OPG1,QQG1,DEF1,OES1, //V,N,CARDNO \$  
 SAVE CARDNO \$  
 COND P2,JUMPPLOT \$  
 PLOT PLTPAR,GPSETS,ELSETS,CASECC,BGPD,EQEXIN,SIL,PUGV1,,GPECT,OES1/  
 PLOTX2/V,N,NSIL/V,N,LUSET/V,N,JUMPPLOT/V,N,PLTFLG/V,N,PFILE \$  
 SAVE PFILE \$

PRTMSG PLOTX2// \$  
LABEL P2 \$  
TA1 ECT,EPT,BGPD,T,SIL,GPDT,CSTM/X1,X2,ECPT,GPCT/V,N,LUSET/ V,N,  
NOSIMP/C,N,0/V,N,NOGENL/V,N,GENEL \$  
DSMG1 CASECC,GPPT,SIL,EDT,UGV,CSTM,MPT,ECPT,GPCT,DIT/KDGG/ V,N,  
DSCOSET \$  
SAVE DSCOSET \$  
CHKPNT KDGG \$  
DPD DYNAMICS,GPL,SIL,USET/GPLD,SILD,USETD,,,,,EED,EQDYN/V,N,  
LUSET/V,N,LUSETD/V,N,NOTFL/V,N,NODLT/V,N,NOPSDL/V,N,NOFRL/ V,  
N,NONLFT/V,N,NOTRL/V,N,NOEED/C,N,/V,N,NOUE \$  
SAVE NOEED \$  
COND ERROR3,NOEED \$  
CHKPNT EED \$  
PARAM //C,N,MPY/V,N,NEIGV/C,N,1/C,N,-1 \$  
LABEL NLVIB \$  
ADD KAA,/KTT/C,N,(-1.0,0.0,0)/C,N,(0.0,0.0,0) \$  
CHKPNT KTT \$  
CEAD KTT,,MAA,EED,CASECC/PHIA,LAMA,OEIGS/S,N,NEIGV \$  
OFF OEIGS,LAMA//S,N,CARDNO \$  
COND ERROR4,NEIGV \$  
SDR1 USET,,PHIA,,GO,GM,,KFS/PHIG,,BOG/1/\*REIG\*/1 \$  
ADD PHIG/PHIAMP/V,Y,AMP \$  
DSMG1 CASECC,,SIL,,PHIAMP,CSTM,MPT,ECPT,GPCT,DIT/KNGG/DSCOSET/1 \$  
CHKPNT KNGG \$  
ADD5 KGG,KDGG,KNGG,, /KSGG \$  
CHKPNT KSGG \$  
EQUIV KSGG,KSNN/MPCF2/MGG,MSNN/MPCF2 \$  
CHKPNT KSNN,MSNN \$  
COND LBL2S,MPCF2 \$  
MCE2 USET,GM,KSGG,MGG/KSNN,MSNN \$  
CHKPNT KSNN,MSNN \$  
LABEL LBL2S \$  
EQUIV KSNN,KSFF/SINGLE/MSNN,MSFF/SINGLE \$  
CHKPNT KSFF,MSFF \$  
COND LBL3S,SINGLE \$  
SCE1 USET,KSNN,MSNN/KSFF,KSFS,,MSFF \$  
CHKPNT KSFF,KSFS,MSFF \$  
LABEL LBL3S \$  
EQUIV KSFF,KSAA/OMIT / MSFF,MSAA/OMIT \$  
CHKPNT KSAA,MSAA \$  
COND LBL5S,OMIT \$  
SMP1 USET,KSFF/GSO,KSAA,KS00,LS00,US00 \$  
SMP2 USET,GSO,MSFF/MSAA \$

```

CHKPNT      KSAA,MSAA $
LABEL       LBL55 $
COPY        KSAA/KAA/IPARM=-1 $
COPY        MSAA/MAA/JPARM=-1 $
REPT        NLVIB,NLOOP $
SDR2        CASECC,CSTM,MPT,DIT,EQEXIN,SIL,,,BGPDT,LAMA,BQG,PHIG,EST,./,
            OBQG1,OPHIG,OBES1,OBEF1,PPHIG/C,N,REIG $
OFF         CPHIG,CBQG1,CBEF1,CBES1,,,//V,N,CARDNO $
SAVE        CARDNO $
COND        P3,JUMPPLOT $
PLOT        PLTPAR,GPSETS,ELSETS,CASECC,BGPDT,EQEXIN,SIL,,,PPHIG,GPECT,
            OBES1/PLOTX3/V,N,NSIL/V,N,LUSET/V,N,JUMPPLOT/V,N,PLTFLG/V,N,
            PFILE $
SAVE        PFILE $
PRTMSG      PLOTX3// $
LABEL       P3 $
JUMP        FINIS $
LABEL       ERROR1 $
PRTPARM     //C,N,-1/C,N,NMDS $
LABEL       ERROR2 $
PRTPARM     //C,N,-2/C,N,NMDS $
LABEL       ERROR3 $
PRTPARM     //C,N,-3/C,N,NMDS $
LABEL       ERROR4 $
PRTPARM     //C,N,-4/C,N,NMDS $
LABEL       ERROR5 $
PRTPARM     //C,N,-5/C,N,NMDS $
LABEL       ERROR6 $
PRTPARM     //C,N,-6/C,N,NMDS $
LABEL       FINIS $
END         $

```

APPENDIX B  
INPUT BULK DATA CARDS

```

$
$ GEOMETRY AND CONSTRAINTS
GRDSET
GRID 1 0.0 246
GRID 2 0.125
GRID 3 0.25
GRID 4 0.375
GRID 5 0.50
GRID 6 0.625
GRID 7 0.75
GRID 8 0.875
GRID 9 1.0
GRID 20 0.0 10.0 123456
SPC 1 1 13 0.0 9 3 0.0
$
$ STRUCTURAL AND AERODYNAMIC ELEMENTS
BAROR 15 20 2
CBAR 1 1 2
CBAR 2 2 3
CBAR 3 3 4
CBAR 4 4 5
CBAR 5 5 6
CBAR 6 6 7
CBAR 7 7 8
CBAR 8 8 9
MAT1* 25 1.0
*MT1 0.4367901341 *MT1
PARAM COUPMASS1
$ DPMN = 2.0*Q/(BETA)
$ WHERE Q = RHO*V**2/2.0, DYNAMIC PRESSURE
$ BETA = SQRT(MACH NO.**2 - 1.0)
PARAM DPMN 600.0
PBAR* 15 25 2.289429 1.0 *PB1
*PB1 1.0
$
$ CONTROL DATA
EIGC 1 INV MAX
+INV1 41.0 -12.0 41.0 -14.0 1.00 1 1 +INV1
$ AMP = AMPLITUDE/SQRT(I/A) = SQRT(12.0)*C/H = SQRT(12.0)*0.6 = 2.078461
$ WHERE I = AREA MOMENT OF INERTIA
$ A = AREA
PARAM AMP 2.0784610.0
PARAM NLOOP 3
$
$ APPLIED INPLANE LOADING
FORCE* 1 9 9.86960440109 +FCE
+FCE -1.0 0.0 0.0
ENDDATA

```

## REFERENCES

1. Fung, Y. C.: On Two-Dimensional Panel Flutter, *J. Aeronautical Sciences*. Vol. 25, 1958, pp. 145-160.
2. Dugundji, J.: Theoretical Considerations of Panel Flutter at High Supersonic Mach Numbers. *AIAA J.*, Vol. 4, 1966, pp. 1257-1266.
3. Dowell, E. H.: A Review of the Aeroelastic Stability of Plates and Shells. *AIAA J.*, vol. 8, 1970, pp. 385-399.
4. Dowell, E. H.: Nonlinear Oscillations of a Fluttering Plate. *AIAA J.* Vol. 4, 1966, pp. 1267-1275.
5. Dowell, E. H. : Nonlinear Oscillations of a Fluttering Plate II. *AIAA J.*, Vol. 5, 1967, pp. 1856-1862.
6. Eastep, F. E. and McIntosh, S. C.: The Analysis of Nonlinear Panel Flutter and Response under Random Excitation or Nonlinear Aerodynamic Loading. *Proceedings AIAA/ASME 11th SDM Conference, Denver, Colo., April 1972*, pp. 36-47.
7. Kuo, C. C., Morino, L. and Dugundji, J.: Perturbation and Harmonic Balance Methods for Nonlinear Panel Flutter. *AIAA J.*, Vol 10, 1972, pp. 1479-1484.
8. Morino, L.: A Perturbation Method for Treating Nonlinear Panel Flutter Problems. *AIAA J.*, Vol. 7, 1969, pp. 405-410.
9. Olson, M.S.: Finite Elements Applied to Panel Flutter. *AIAA J.* Vol. 5, 1967, pp. 2267-2270.
10. Kariappa and Somashekar, B.R.: Application of Matrix Displacement Methods in the Study of Panel Flutter. *AIAA J.*, Vol. 7, 1969, pp. 50-53.
11. Olson, M.S.: Some Flutter Solutions Using Finite Elements. *AIAA J.*, Vol. 8, 1970, pp. 747-752.
12. Kariappa, Somashekar, B. R. and Shah, C. G.: Discrete Element Approach to Flutter of Skew Panels with In-plane Forces under Yawed Supersonic Flow. *AIAA J.*, Vol. 8, 1970, pp. 2017-2022.
13. Sander G., Bon C. and Geradin, M.: Finite Element Analysis of Supersonic Panel Flutter. *Int. J. Numerical Methods in Engr.*, Vol. 7, 1973, pp. 379-394.

## REFERENCES (CONT'D)

14. Rossettos, J. N. and Tong, P.: Finite-Element Analysis of Vibration and Flutter of Cantilever Anisotropic Plates. ASME Paper 74-WA/APM-15.
15. Bismarck-Nasr, M. N.: Finite Element Method Applied to the Supersonic Flutter of Circular Cylindrical Shells. Int. J. Numerical Methods in Engr., Vol. 10, 1976, pp. 423-435.
16. Mei, C.: Finite Element Displacement Method for Large Amplitude Free Flexural Vibrations of Beams and Plates. Int. J. Comp. & Stru., Vol. 3, 1973, pp. 163-174.
17. Mei, C. and Rogers, J. L., Jr.: NASTRAN Nonlinear Vibration Analysis of Beam and Frame Structures. NASA TM X-3278, 1975, pp. 259-284.
18. Rao, G. V., Raju, I. S. and Raju, K. K.: Nonlinear Vibrations of Beams Considering Shear Deformation and Rotatory Inertia. AIAA J., Vol. 14, 1976, pp. 685-687.
19. Bergan, P. G. and Clough, R. W.: Convergence Criteria for Iterative Processes. AIAA J., Vol. 10, 1972, pp. 1107-1108.
20. Olson, M. D.: On Applying Finite Elements to Panel Flutter. Aero. Rept. LR-476, National Research Council, Ottawa, Canada, March 1967.
21. Ray, J. D. and Bert, C. W.: Nonlinear Vibrations of a Beam with Pinned Ends. Trans. ASME, J. Engr. for Industry, Vol. 91, 1969, pp. 997-1004.

TABLE 1. IN VACUO EIGENVALUES AND COALESCENCE RESULTS  
FOR SIMPLY SUPPORTED AND CLAMPED PANELS

<u>Simply Supported Panel</u>				
Number of Elements	In Vacuo		Coalescence	
	$\kappa_1$	$\kappa_2$	$\lambda_{cr}$	$\kappa_{cr}$
2	98.1795	1920.00	398.536	1206.32
4	97.4597	1570.87	342.347	1043.47
8	97.4123	1559.35	343.280	1051.22
Exact (ref. 20)	97.4091	1558.55	343.3564	1051.797

<u>Clamped Panel</u>				
Number of Elements	In Vacuo		Coalescence	
	$\kappa_1$	$\kappa_2$	$\lambda_{cr}$	$\kappa_{cr}$
2	516.923	6720.00	922.388	3618.46
4	501.894	3874.23	636.437	2721.38
8	500.648	3808.34	636.586	2740.16
Exact (ref. 20)	500.564	3803.54	636.5691	2741.360

TABLE 2. EFFECT OF AMPLITUDE RATIO ON IN-VACUO FREQUENCY RATIOS  
 $(\omega/\omega_0)_n$  FOR SIMPLY SUPPORTED PANEL

Amplitude $(\frac{c}{h})$	Mode n	Number of Elements			Theory (ref. 21)		
		4	8	12	Assumed Space Mode	Assumed Time Mode	Galerkin
0.0	1	1.000	1.000	1.000	1.000	1.000	1.000
	2	1.004	1.000	1.000	1.000	-	-
0.2	1	1.038	1.039	1.040	1.056	1.032	1.048
	2	1.030	1.038	1.039	1.056	-	-
0.4	1	1.141	1.147	1.148	1.206	1.124	1.181
	2	1.106	1.141	1.146	1.206	-	-
0.6	1	1.292	1.304	1.306	1.411	1.262	1.375
	2	1.221	1.292	1.301	1.411	-	-
0.8	1	1.471	1.489	1.492	1.647	1.434	1.607
	2	1.367	1.471	1.484	1.647	-	-
1.0	1	1.667	1.690	1.693	1.902	1.627	1.863
	2	1.534	1.667	1.685	1.902	-	-
1.2	1	1.869	1.902	1.906	2.167	1.837	2.136
	2	1.716	1.870	1.895	2.167	-	-



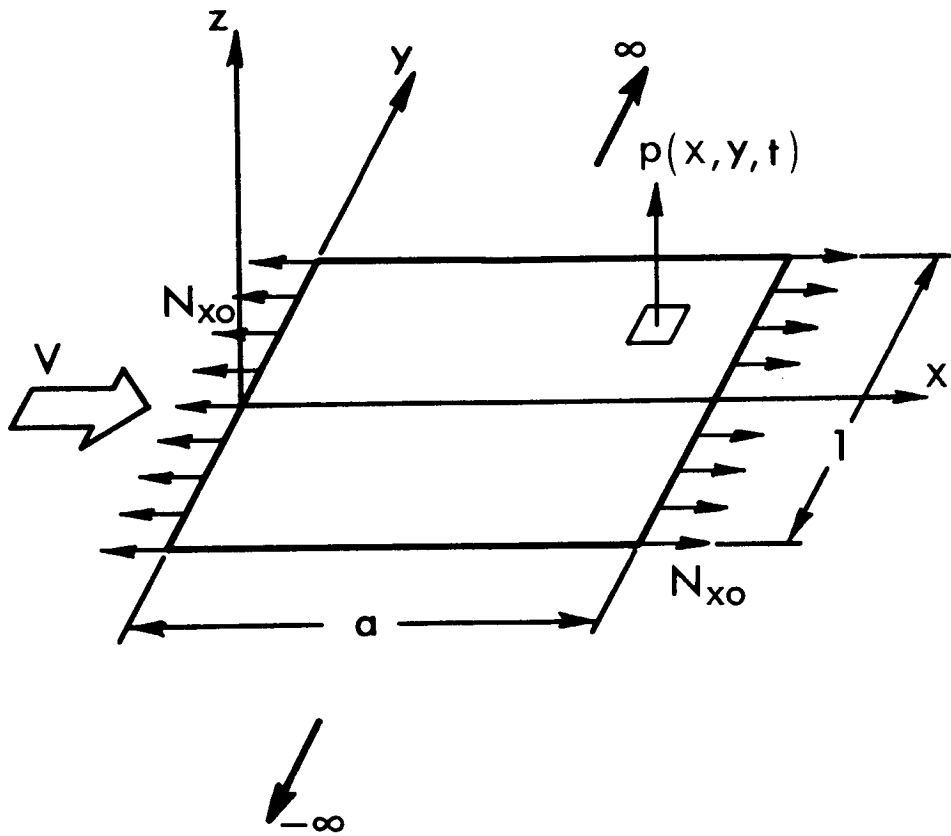


Figure 1. Panel geometry.

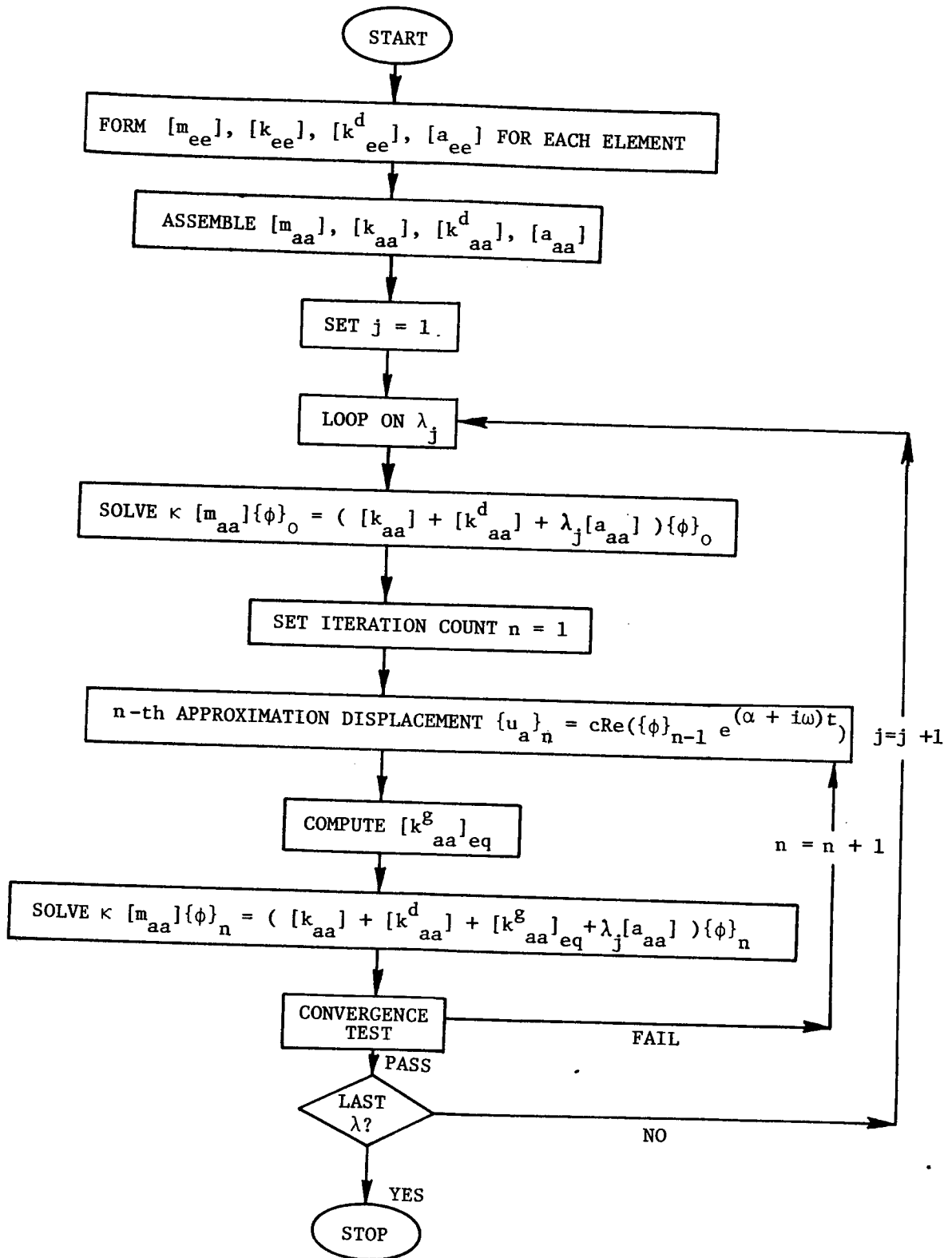


Figure 2. Simplified flow diagram for large deflection panel flutter analysis.

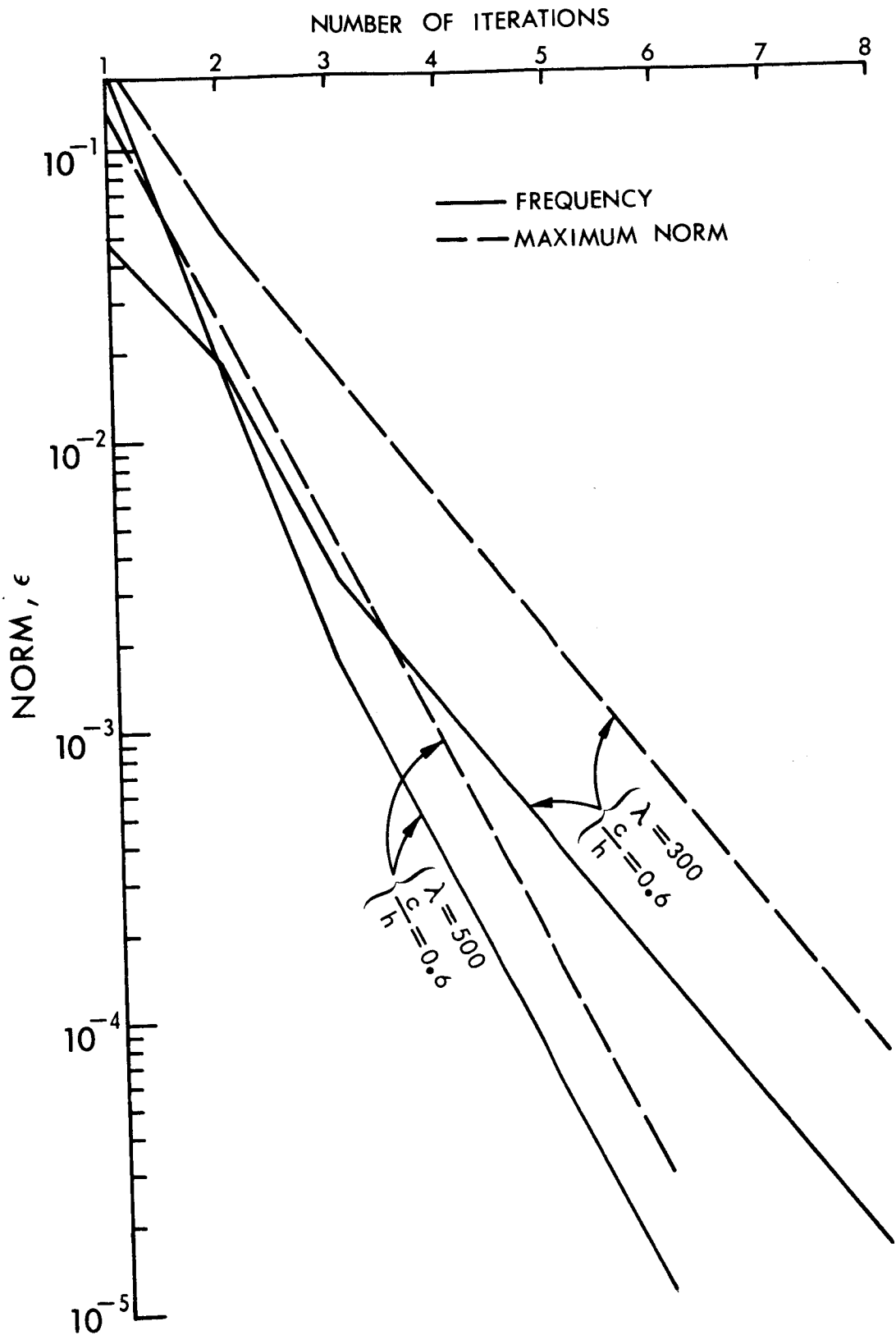


Figure 3. Convergence characteristics.

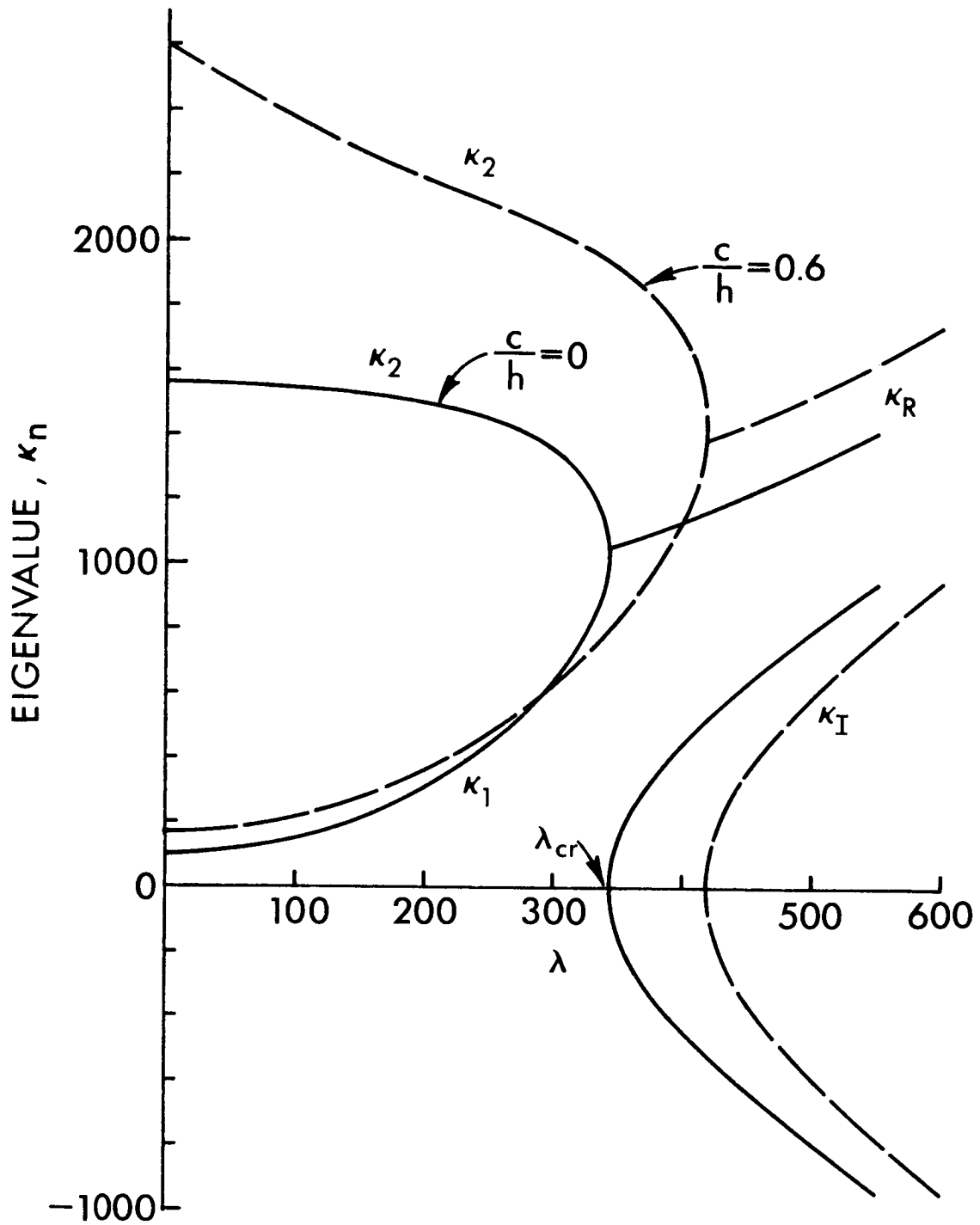


Figure 4. Variation of eigenvalues with dynamic pressure for simply supported panel ( $N_{x0} = 0$ ).

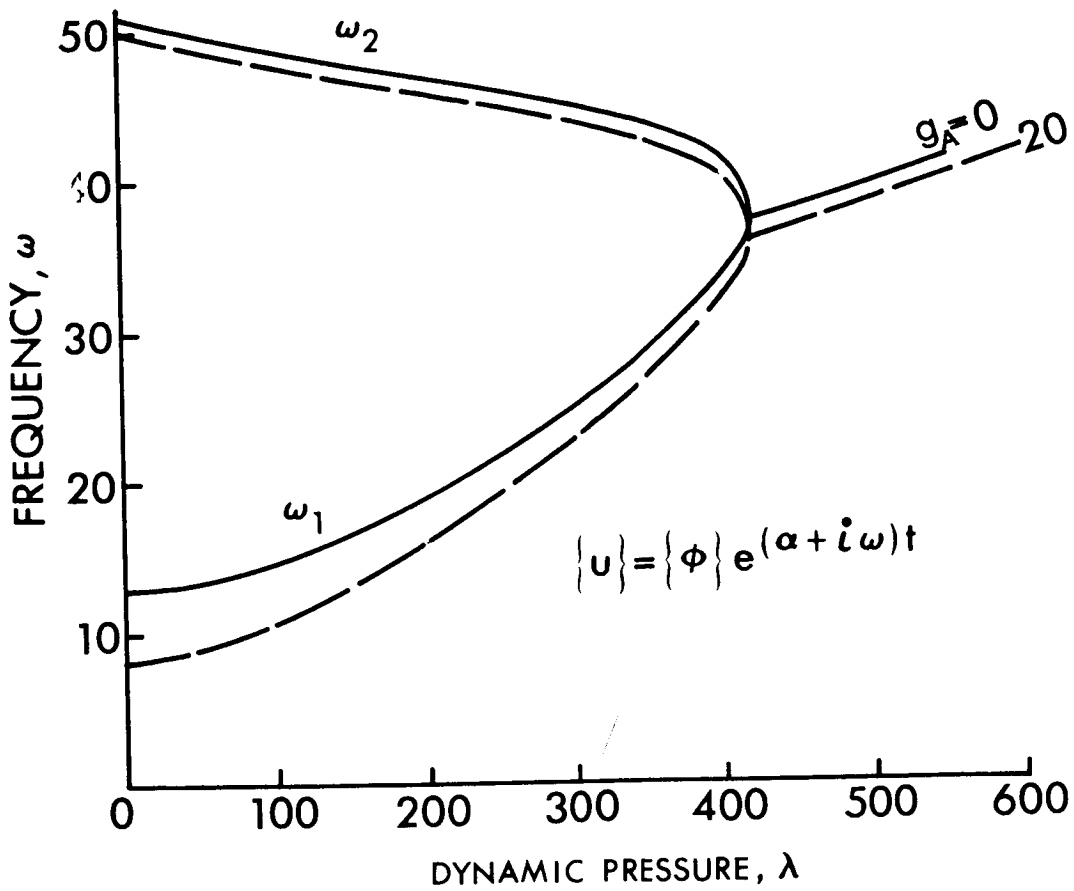
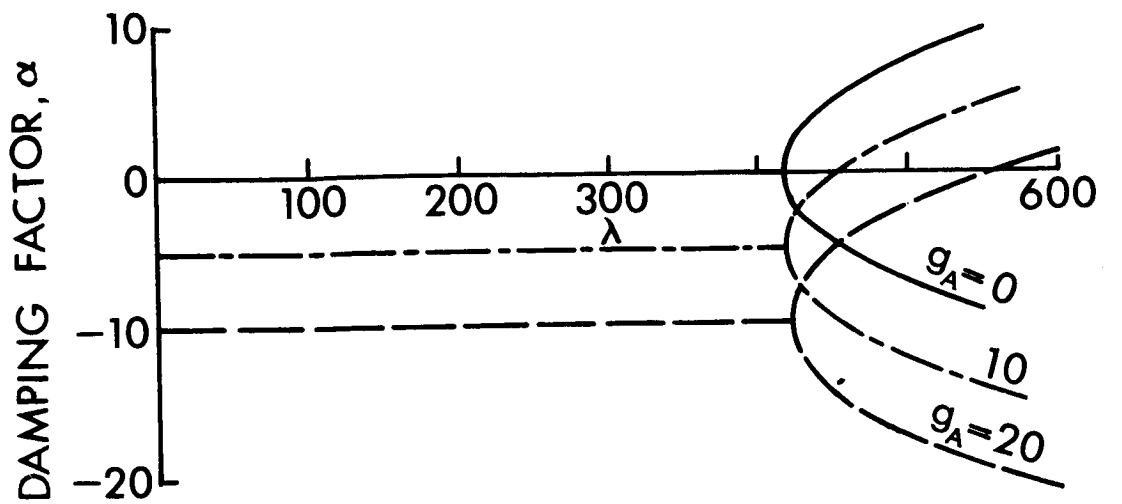


Figure 5. Typical plots of panel behavior and effect of aerodynamic damping (simply supported panel,  $\frac{c}{h} = 0.6$  and  $N_{x0} = 0$ ).

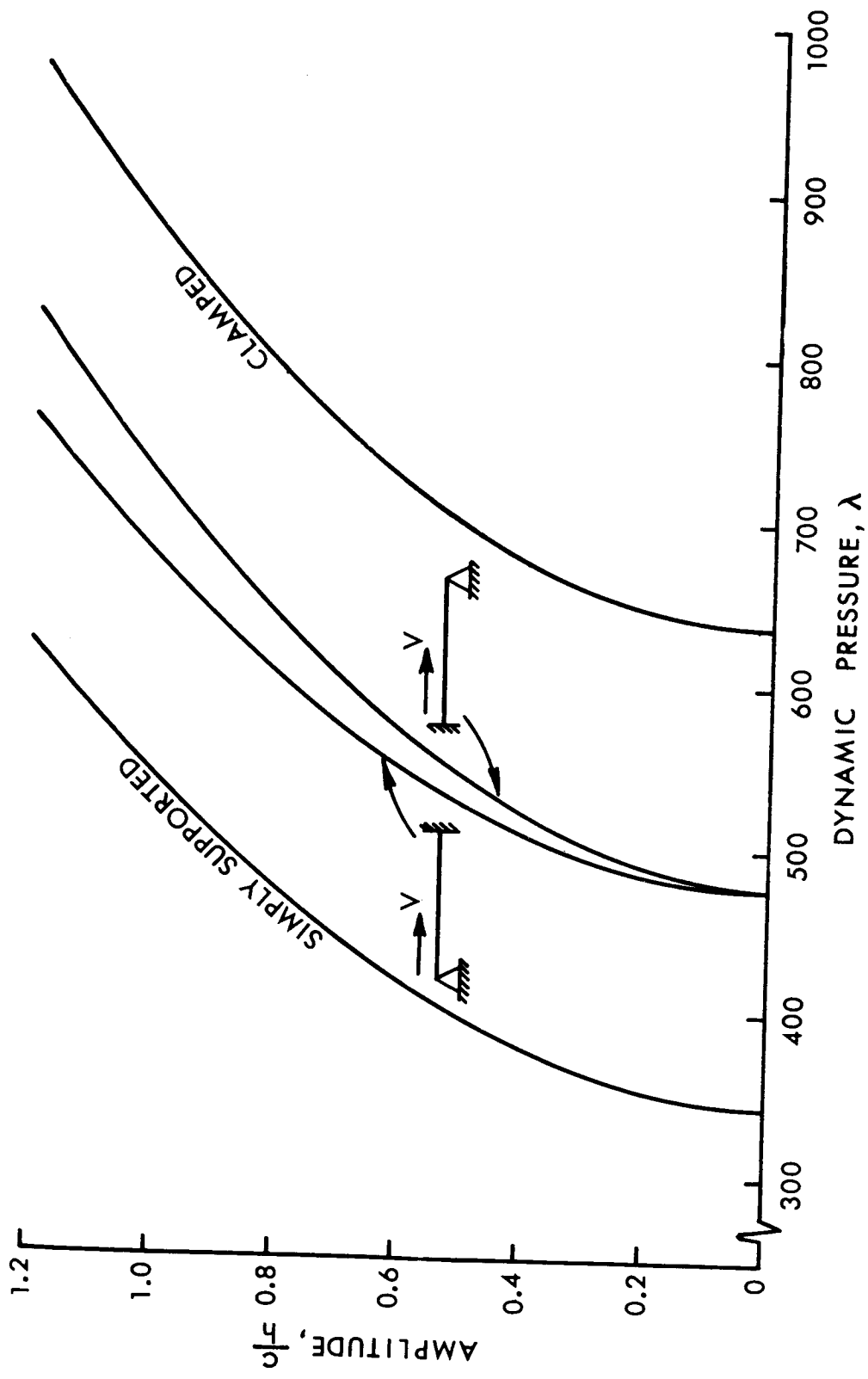


Figure 6. Limit cycle amplitude versus dynamic pressure for panels with various support conditions ( $N_{x0} = g_A = 0$ ).

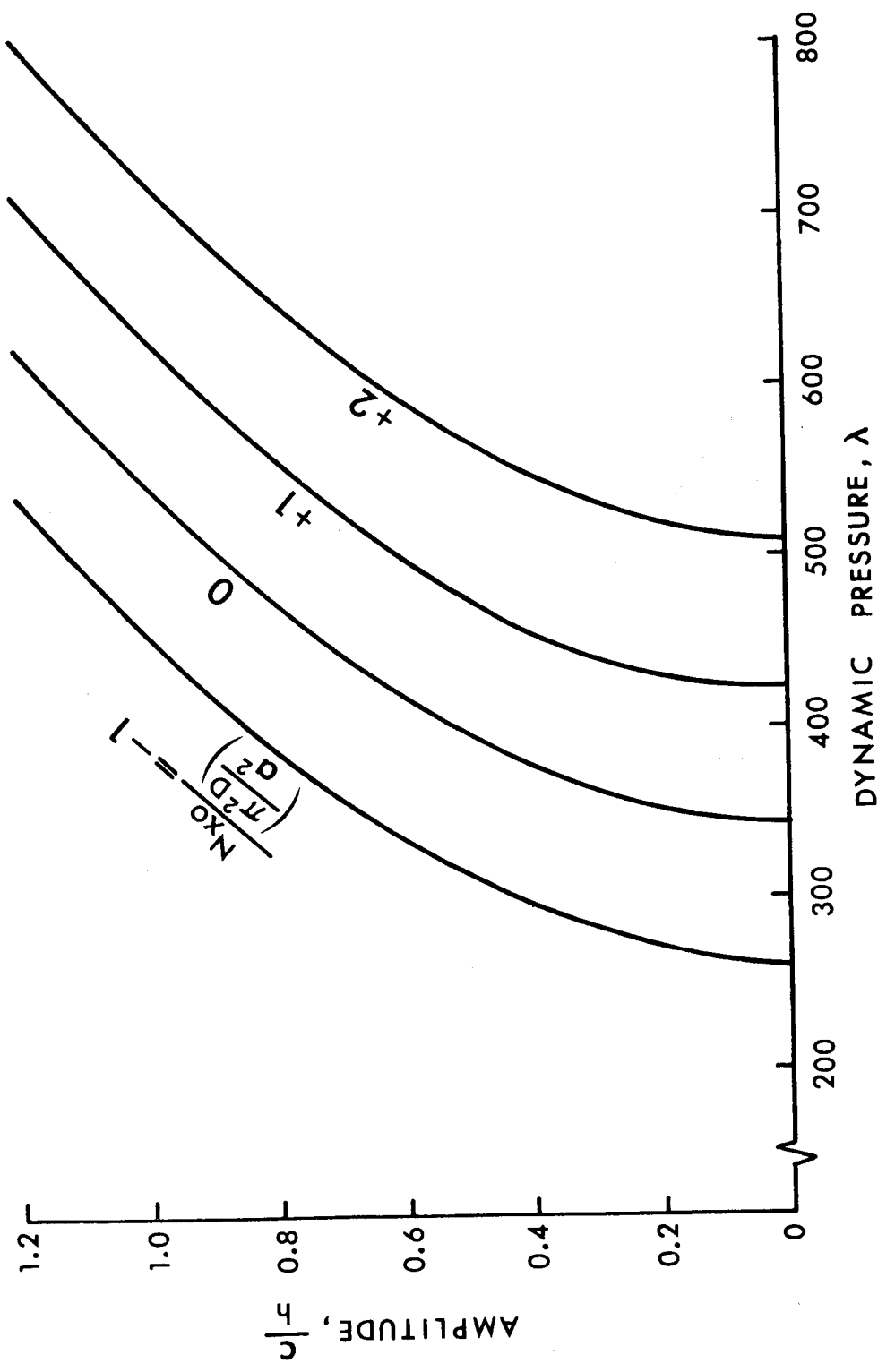


Figure 7. Limit cycle amplitude versus dynamic pressure for simply supported panel under different in-plane forces ( $g_A = 0$ ).